Soft Matter

A simple strategy to improve the interfacial activity of true Janus gold nanoparticles: a shorter hydrophilic capping ligand†

Miguel Angel Fernandez-Rodriguez,[a] Limei Chen,[b] Christopher P. Deming,[b] Miguel Angel Rodriguez-Valverde,[a] Shaowei Chen,[b] Miguel Angel Cabrerizo-Vilchez[a] and Roque Hidalgo-Alvarez*[a]

Janus gold nanoparticles (JPs) of ∼4 nm-diameter half functionalized with 1-hexanethiol as a hydrophobic capping ligand exhibit significantly higher interfacial activity, reproducibility and rheological response when the other half is functionalized with 1,2-mercaptopropanediol (JPs-MPD) than with 2-(2-mercaptoethoxy)ethanol (JPs-MEE), both acting as hydrophilic capping ligands. The interfacial pressure measured by pendant drop tensiometry reaches 50 mN m^{-1} and 35 mN m^{-1} for the JPs-MPD at the water/air and water/decane interface, respectively. At the same area per particle, the JPs-MEE reveal significantly lower interfacial pressure: 15 mN m^{-1} and 5 mN m^{-1} at the water/air and water/decane interface, respectively. Interfacial dilatational rheology measurements also show an elastic shell behaviour at higher compression states for JPs-MPD while the JPs-MEE present near-zero elasticity. The enhanced interfacial activity of JPs-MPD is explained in terms of chemical and hydration differences between the MPD and MEE ligands, where MPD has a shorter hydrocarbon chain and twice as many hydroxyl terminal groups as MEE.

Pickering emulsions can be thermodynamically stabilized by amphiphilic Janus nanoparticles (JPs) with a wettability anisotropy.[1–3] It is known that JPs show three times more adsorption energy than homogeneous nanoparticles.[2,4] Much effort has been made to synthesize and simulate JPs with different morphologies and surface chemistry to control the way in which these particles self-assemble at fluid interfaces.[5–9]

Gold nanoparticles randomly functionalized with 1-undecanethiol and *N*,*N*,*N*-trimethyl (11-mercaptoundecyl) ammonium chloride are reported to become Janus-like when the capping ligands rearrange themselves at the water/air interface.[10] Nevertheless, recently Reguera *et al.*[11] demonstrated by neutron

reflectivity that such a rearrangement does not happen with gold nanoparticles functionalized with 1-octanethiol and 6-mercapto-1-hexanol at the water/air interface. One way of obtaining gold JPs with true separate domains is to selectively functionalize each hemisphere of the core with the desired capping ligands immobilizing the nanoparticles using a Langmuir balance.[12,13]

It is fundamental to select appropiate capping ligands that will confer Janus character to the nanoparticles because of the significant dependence between these capping ligands and the interfacial activity of the final JPs. We propose a simple strategy to enhance the interfacial activity, rheological response and reproducibility through the colloidal stability of true gold Janus nanoparticles. We synthesized Janus gold nanoparticles half capped by 1-hexanethiol and the other half by 2-(2-mercaptoethoxy)ethanol (JPs-MEE) or 1,2-mercaptopropanediol (JPs-MPD) under surfactant-free conditions as described in previous studies (see Fig. 1).[12–14] The sizes obtained by high resolution TEM measurements (see Fig. S1†) are 3.5 ± 0.9 nm and 3.7 ± 1.9 nm for the JPs-MEE and JPs-MPD, respectively. The electrophoretic mobilities of both JPs were measured using a ZetaSizer Nano (Malvern) in a 10^{-2} M sodium citrate MilliQ water solution to stabilize the electrical double layer obtaining $\mu_{e,\text{JPs-MEE}} = (-2.2 \pm 1.5) \times 10^{-8}$ m^2 V^{-1} s^{-1} and $\mu_{e,\text{JPs-MPD}} = (-2.9 \pm 0.4) \times 10^{-8}$ m^2 V^{-1} s^{-1}. From previous studies, the JPs-MEE showed an average macroscopic contact angle of $(56.1 \pm 1.8)°$ and $(49.0 \pm 1.3)°$ in each hemisphere, whereas the JPs-MPD showed $(63.3 \pm 2.7)°$ and $(53.4 \pm 2.9)°$ in their hydrophobic and hydrophilic hemispheres, respectively.[12,13] The contact angles are slightly lower for the JPs-MEE likely due to the fabrication

[a] *Biocolloid and Fluid Physics Group, Applied Physics Department, Faculty of Sciences, University of Granada, Granada, Spain. E-mail: rhidalgo@ugr.es*

[b] *Department of Chemistry and Biochemistry, University of California, 1156 High Street, Santa Cruz, CA 95064, USA*

† Electronic supplementary information (ESI) available: HRTEM micrographs and pendant drop pictures. See DOI: 10.1039/c5sm01908g
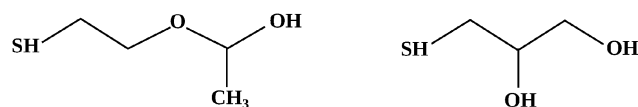

Fig. 1 MEE (left) and MPD (right) capping ligands. The SH group is the anchor group at the gold nanoparticle surface.
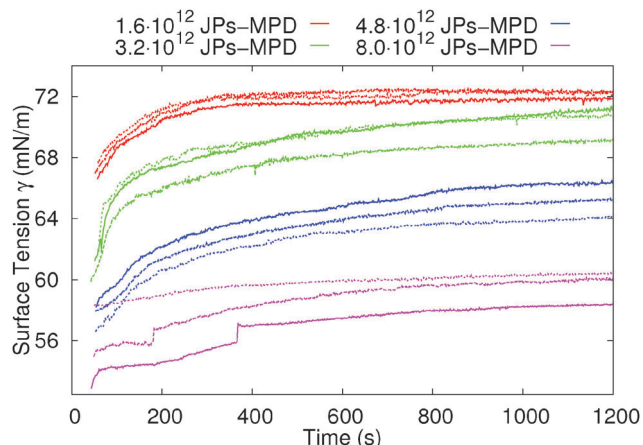
Fig. 2 Surface tension evolution over the time after the deposition of different numbers of JPs-MPD in THF on the surface of an initial 5 µL MilliQ water pendant drop and growth up to 45 µL. The same color curves correspond to different experiments with the same number of deposited JPs-MPD. After the solvent evaporation, the surface tension remained stable.

process: for MEE adsorption, the close-packed monolayer of 1-hexanethiol covered gold nanoparticles was immersed in a water solution containing MEE[13] and this might produce greater hydrophilic capping ligand exchange and thus a lower contact angle than that for the JPs-MPD in which the functionalization with MPD was performed directly using a Langmuir balance, exchanging the MPD ligands from the water subphase.[12] The contact angle values in the hydrophilic hemispheres are similar within errors, which reflects that the differences between MPD and MEE are not reflected macroscopically in the contact angle and the wettability contrast (i.e. contact angle differences between hemispheres) is similar in both JPs-MEE and JPs-MPD within errors. The pendant drop tensiometry was conducted as follows: different amounts of Janus nanoparticles (JPs-MEE and JPs-MPD) dispersed in tetrahydrofuran (THF, HPLC grade) were deposited on a water pendant drop using a handheld micro-syringe and a micropositioner. The surface tension was obtained

by axisymmetric drop shape analysis upon THF evaporation, while the pendant drop volume was kept constant. The results in Fig. 2 show a decrease in the final surface tension after evaporation of THF which is higher as the concentration of JPs-MPD is increased (refer to previous work for a similar characterization of the JPs-MEE[15]). The experiments are highly reproducible as can be seen from the different runs for a fixed concentration of JPs (different curves with the same color in Fig. 2).

After the THF evaporation, growing and shrinking experiments were performed at 0.08 µL s^{-1} for each JP concentration. Next, the pendant drop was immersed in decane and the growing and shrinking experiments were performed again. We plot the interfacial pressure ($\Pi = \gamma_0 - \gamma$, where γ_0 is 72.5 mN m^{-1} for the water/air (W/A) and 52.3 mN m^{-1} for the water/decane (W/O) interfaces and γ is the measured interfacial tension) against the drop area per particle (A_p, the area of the pendant drop divided by the number of deposited JPs). A piecewise compression isotherm can be seen in Fig. 3a and b for W/A and W/O interfaces, respectively. The first remarkable fact is the lower interfacial activity of JPs-MEE compared to JPs-MPD at the same A_p values. At the lowest A_p value reached for JPs-MPD, Π is 50 mN m^{-1} and 35 mN m^{-1} and 15 mN m^{-1} and 5 mN m^{-1} for the JPs-MEE at the W/A and W/O interfaces, respectively. The highest Π values obtained for JPs-MEE, after further compression, are 30 mN m^{-1} and 20 mN m^{-1} at the W/A and W/O interfaces, respectively. Contrary to JPs-MEE, the compression isotherms for JPs-MPD at the W/A interface exhibit open cycles at the beginning of the experiments indicating that the colloidal monolayer rearranges itself into a final state that is preserved in further compression cycles. This behaviour is attenuated at the W/O interface as the hysteresis cycles are much smaller (i.e. the upper compression and lower expansion curves are closer) which might be due to the fact that enough energy is provided to reach a more relaxed state when it is immersed in decane. Moreover, the low hysteresis of the JPs-MEE compression cycles compared to the JPs-MPD might be due to the lower interfacial activity of these particles. Since the fabrication process, hydrophobic capping

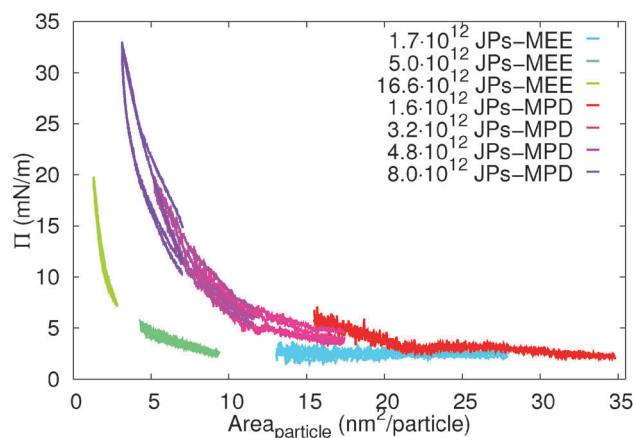(a) Water/air interface
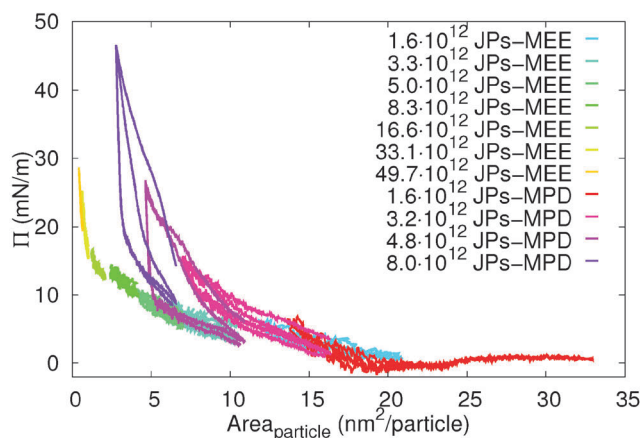
(b) Water/decane interface

Fig. 3 Surface pressure against the area per particle for different numbers of JPs-MEE and JPs-MPD deposited at the (a) W/A and (b) W/O interfaces. For a more detailed characterization of the JPs-MEE, please refer to Fernandez et al.[15]

ligand, wettability contrast, size and charge were similar for both JPs-MEE and JPs-MPD, the differences between interfacial activity must arise from the interfacial activity of the MEE and MPD hydrophilic capping ligands. Whereas MEE has a longer hydrocarbon chain (four CH_2 and one oxygen) and one hydroxyl terminal group, the MPD has a shorter hydrocarbon chain (three CH_2) and two hydroxyl terminal groups (see Fig. 1). The lower number of hydrocarbon groups and higher number of hydroxyl groups of MPD might result in higher hydration of the hydrophilic hemisphere of the JPs (*i.e.* establishing hydrogen bonds between water and the hydrophilic capping ligands). These chemical differences might play a decisive role in the final interfacial activity of these JPs.

The interfacial dilatational rheology of the JPs was evaluated by ten periodic volume variations of 1 μL at different periods. When the pendant drop is subjected to a periodic injection/extraction of volume, the interface tries to re-establish the equilibrium. This counteraction is represented by a complex quantity composed of a storage part and a loss part:

$$E = E_d + i\omega\eta_d \tag{1}$$

where E is the surface dilatational modulus that accounts for the change in surface tension produced by a small change in the surface area, E_d is the interfacial dilatational elasticity, ω is the oscillation frequency and η_d is the interfacial dilatational viscosity.[16] If the viscosity is negligible during the relaxation process after perturbation of the interface, the interface presents an essentially elastic behavior. The extraordinary interfacial activity of JPs-MPD is reflected in the rheology results shown in Fig. 4a and b (see Fig. S2 and S3†). For both W/A and W/O interfaces, E decreases slightly and η increases for increasing periods. For the W/A interface, E_d and η_d increase clearly with the compression state of the colloidal monolayer. This trend is also observed for the W/O interface but with lower values for both E_d and η_d. The high E_d value is an indication that the colloidal monolayer creates an elastic shell on the pendant drop at higher compression states. This elastic behaviour again suggests the ability of the JPs-MPD as emulsifiers. Further rheology experiments were performed for a fixed period of 10 s comparing the response of JPs-MEE and JPs-MPD. The results in Fig. 4c and d indicate that the JPs-MPD
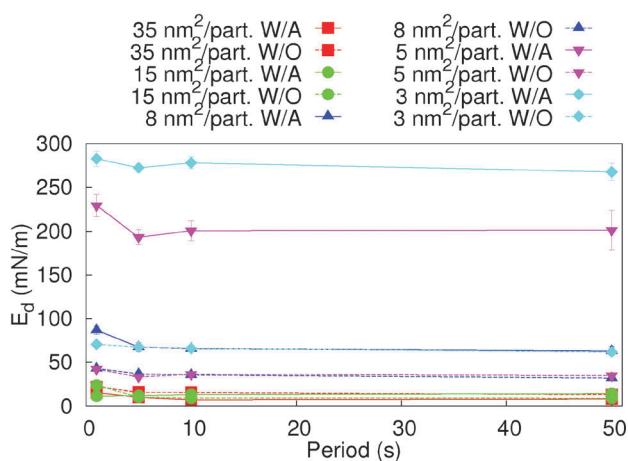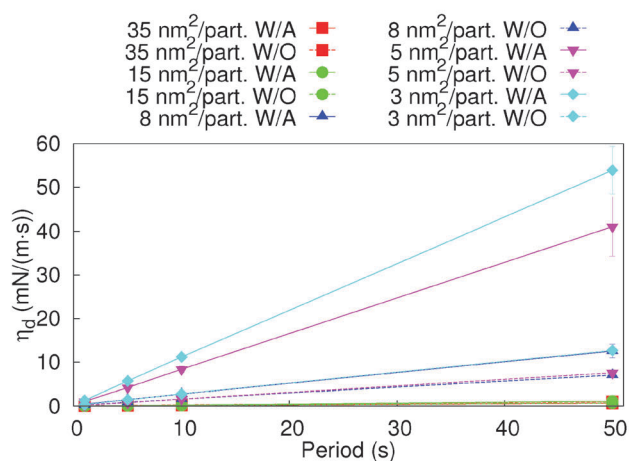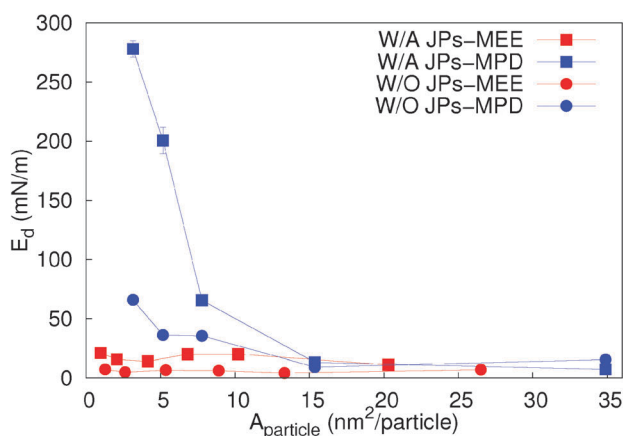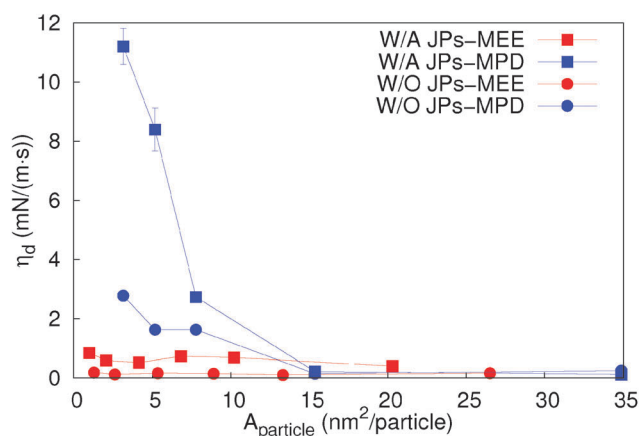

Fig. 4 (a) Interfacial dilatational elastic modulus (E_d) and (b) viscosity (η_d) of JPs-MPD against different periods for different A_p compression states at the W/A and W/O interfaces. (c) E_d and (d) η_d of JPs-MEE and JPs-MPD against the A_p at the W/A and W/O interfaces, for a 10 s period.

reach significantly higher E_d and η_d values upon compression (*i.e.* lower A_p) than the JPs-MEE ($\sim$10 times higher E_d and η_d for JPs-MPD than JPs-MEE at the W/A interface and 2 times at the W/O interface), suggesting that the elastic shell behaviour is not exhibited by the JPs-MEE. A final consideration must be taken into account for gold nanoparticles in the range of a few nanometers (*i.e.* less than 10 nm), where the adsorption energy at the interface is of the order of $K_B T$[17] and they are expected to easily leave the interface. Nevertheless, the stable interfacial tension over time after the THF evaporation, the closed growing/shrinking cycles and the dilatational rheology seem to indicate that the JPs-MEE and JPs-MPD are irreversibly anchored at the W/A and W/O interfaces, probably due to their Janus character.

In conclusion, the JPs-MEE and JPs-MPD are similar in fabrication process, hydrophobic capping ligand, wettability contrast, size and charge, but are functionalized with different hydrophilic capping ligands. The JPs-MPD exhibit a significantly higher interfacial activity at the W/A and W/O interfaces. Moreover, the dilatational rheology suggests an elastic shell-like behaviour of the pendant drop when the JPs-MPD are deposited at the W/A and W/O interfaces. This elastic shell behaviour seems to be absent in the JPs-MEE. This points out the importance of the chemical structure of the capping ligands in JPs to predict the interfacial activity and therefore their ability as emulsifiers. A shorter hydrocarbon chain and more hydroxyl terminal groups in the hydrophilic capping ligands seem to be a route to obtain enhanced interfacial activity of this kind of JP *via* enhanced hydration of the hydrophilic hemisphere of the JPs. To the best of our knowledge, this is the first time that such high interfacial activity has been obtained with 4 nm-diameter gold nanoparticles under surfactant-free conditions.

Acknowledgements

References

1 J. Hu, S. Zhou, Y. Sun, X. Fang and L. Wu, *Chem. Soc. Rev.*, 2012, **41**, 4356–4378.
2 A. Kumar, B. J. Park, F. Tu and D. Lee, *Soft Matter*, 2013, **9**, 6604–6617.
3 B. T. T. Pham, C. H. Such and B. S. Hawkett, *Polym. Chem.*, 2015, **6**, 426–435.
4 R. Aveyard, *Soft Matter*, 2012, **8**, 5233–5240.
5 A. Walther and A. H. E. Muller, *Janus Particle Synthesis, Self-Assembly and Applications*, The Royal Society of Chemistry, 2012, pp. 1–28.
6 J. Du and R. K. O'Reilly, *Chem. Soc. Rev.*, 2011, **40**, 2402–2416.
7 B. J. Park, T. Brugarolas and D. Lee, *Soft Matter*, 2011, **7**, 6413–6417.
8 H. Rezvantalab and S. Shojaei-Zadeh, *Soft Matter*, 2013, **9**, 3640–3650.
9 Z.-W. Li, Z.-Y. Lu, Z.-Y. Sun and L.-J. An, *Soft Matter*, 2012, **8**, 6693–6697.
10 Y. Song, X. Liu and S. Chen, *Functional Nanometer-Sized Clusters of Transition Metals: Synthesis, Properties and Applications*, The Royal Society of Chemistry, 2014, pp. 407–433.
11 J. Reguera, E. Ponomarev, T. Geue, F. Stellacci, F. Bresme and M. Moglianetti, *Nanoscale*, 2015, **7**, 5665–5673.
12 S. Pradhan, L. Xu and S. Chen, *Adv. Funct. Mater.*, 2007, **17**, 2385–2392.
13 S. Pradhan, L. Brown, J. Konopelski and S. Chen, *J. Nanopart. Res.*, 2009, **11**, 1895–1903.
14 Y. Song and S. Chen, *Chem. – Asian J.*, 2014, **9**, 418–430.
15 M. A. Fernandez-Rodriguez, Y. Song, M. A. Rodriguez-Valverde, S. Chen, M. A. Cabrerizo-Vilchez and R. Hidalgo-Alvarez, *Langmuir*, 2014, **30**, 1799–1804.
16 K. C. Powell and A. Chauhan, *Langmuir*, 2014, **30**, 12287–12296.
17 S. Jiang and S. Granick, *Janus Particle Synthesis, Self-Assembly and Applications*, The Royal Society of Chemistry, 2012, pp. 244–256.